Precision QCD Measurements at HERA

Karin Daum[1,2,3]

[1]Bergische Universität Wuppertal, Guaßstraße 20, 42097 Wuppertal, Germany
[2] also at DESY, Notkestraße 85, 22607 Hamburg, Germany
[3]*On behalf of the H1 and ZEUS collaborations*

DOI: will be assigned

Recent QCD results obtained by the H1 and ZEUS collaborations at the *ep* collider HERA are presented. The high precision measurements of the inclusive deep-inelastic scattering cross section at high photon virtualities Q^2 are used to search for signs of physics beyond the Standard Model. The studies of hadronic final states such as diffraction, jet and heavy quark production as well as particle production are summarised. Predictions from perturbative QCD are confronted with these measurements and the consistency of the understanding of strong interactions tested by these processes is discussed.

1 Introduction

HERA was operated during the years 1992 to 2007 producing ep[1] interactions at centre-of-mass energies up to $\sqrt{s} = 320$ GeV. Both collider experiments H1 and ZEUS collected data corresponding to an integrated luminosity of 0.5 fb^{-1} each.

The HERA collider was an unique machine for studying strong interactions. It provides a clean environment for the precise determination of the proton structure over a wide range in Bjorken x and in virtuality Q^2 of the exchanged boson, which is either a photon or a Z-boson in case of neutral current (NC) interaction, $ep \to eX$, or a W-boson in case of charged current (CC) interactions, $ep \to \nu X$. The two high resolution multi-purpose detectors H1 and ZEUS allow for detailed analyses of the hadronic final state and thereby give access to the vast physics of diffraction and of jet, heavy quark and particle production. By all these processes different aspects of strong interactions are addressed making HERA an ideal testing ground for QCD. This talk will focus on application of parton distribution functions ($PDFs$) of the proton in searches for signals of new physics at HERA, on the strong coupling constant α_S and on fragmentation functions (FFs).

A precise knowledge of the proton PDFs is vital for interpreting the data taken at hadron colliders, especially when analysing rare Standard Model (SM) processes or when searching for signs of new physics. The backbone of all modern proton PDFs [1, 2, 3, 4, 5] are the proton structure function data from HERA [6]. In the determination of PDFs the understanding of charm production is of utmost importance. Not only that charm production contributes up to 30% to the inclusive NC cross section at HERA but also that the treatment of heavy flavour production in the calculations is a theoretical issue due to the presence of several hard scales in the problem and gives therefore rise to different PDF schemes [1, 2, 5].

[1]The term *electron* is used generically for both electrons or positrons if not otherwise stated.

The strong coupling constant α_S is a free parameter in QCD which has to be determined experimentally. Different processes are investigated to measure α_S [7], all having some experimental and/or theoretical challenges. At HERA the study of jet production with sufficiently high transverse jet momenta p_T^{jet} is best suited for the determination of α_S.

The basic concept of pQCD tightly relates the QCD evolution of PDFs to that of FFs [8] which means that the QCD vacuum as seen by studying the structure of the proton is identical to the vacuum acting in the formation of hadrons. Information on the fragmentation functions are obtained from the analysis of particle production mainly in e^+e^--annihilation. The study of particle production in ep-scattering at HERA allows testing the universality of FFs.

2 Search for physics beyond the Standard Model

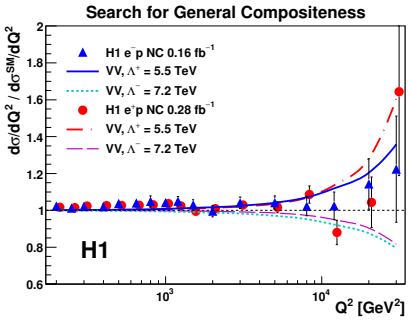

Figure 1: NC cross section $\mathrm{d}\sigma/\mathrm{d}Q^2$ normalised to the SM expectation. The H1 data are compared with the 95% C.L. limit curves for the VV compositeness scale model.

The preliminary HERA combined inclusive measurements based on the full data sets [9] are discussed in the context of the proton structure elsewhere [6]. The measured cross sections are very well described over four orders of magnitude in Q^2 and x by the SM also when using PDFs not fitted to these data. Any contribution from new physics to the DIS cross section should show up in deviations from the SM expectation. All results presented in this section are based on the full statistics taken by the experiments.

Different approaches are followed when searching for signs of new physics at HERA. The most general ansatz presented here is the search for contact interactions (CI). New phenomena with scales above the direct reach of HERA may contribute at lower scales via four-fermion-interactions[2] leading to deviations of the cross section from the SM expectation at large Q^2. This strategy allows different models of new physics to be tested. The procedure has been recently applied by H1 [10] to set lower limits on compositeness scales, on masses of heavy leptoquarks (LQ), on the gravitational scale in large extra dimensions and to set an upper limit on the quark radius. In Figure 1 the NC $e^{\pm}p$ cross sections $\mathrm{d}\sigma/\mathrm{d}Q^2$ normalised to the SM expectations are compared to the prediction corresponding to the 95% C.L. lower limits of the VV compositeness model, $\Lambda^+_{VV} > 5.6$ TeV and $\Lambda^-_{VV} > 7.2$ TeV.

Lower mass limits on heavy leptoquarks are also derived from dedicated searches for first generation LQs [11, 13], $ep \to LQ \to e(\nu)X$, as well as for lepton-flavour violating (LFV) LQs [12], $ep \to LQ \to \mu(\tau)X$. In both cases LQs may be produced either in the s-channel, leading to high sensitivity to the LQ-coupling λ_{LQ} for LQ masses M_{LQ} below the kinematic limit of HERA, $M_{LQ} \leq \sqrt{s}$, or in the u-channel which enables the search for LQs with $M_{LQ} > \sqrt{s}$ and larger values of λ_{LQ}. The searches are performed for both scalar (S) and vector-type (V) LQs.

In Fig. 2 the exclusion curves at 95% C.L. are shown for different first generation V-type LQs in the BRW model [14] in the M_{LQ}-λ_{LQ}-plane from ZEUS (preliminary). Depending on the LQ type lower mass limits up to 630 GeV (ZEUS) and 800 GeV (H1) are obtained assuming

[2] This concept was originally introduced in the Fermi theory of β decay.

a coupling λ_{LQ} of electromagnetic coupling strength ($\lambda_{LQ} = 0.3$). For LQs coupling also to neutrinos the limits obtained in the direct search are in general superior to those obtained by the CI analysis, because both NC and CC data are used.

While the search for first generation LQ is based on finding deviations from the SM in the measured inclusive NC (and CC) cross section the search for LFV LQs requires a dedicated analysis of the final state to identify individual LQ candidates. Event topologies consistent with the LQ hypothesis are selected containing exactly one high p_T well isolated muon or τ-candidate and a single high p_T jet. In the H1 analysis lower limits on M_{LQ} up to 712 GeV and 479 GeV are obtained at 95% C.L. for second or third generation LQs, respectively, assuming $\lambda_{LQ} = 0.3$.

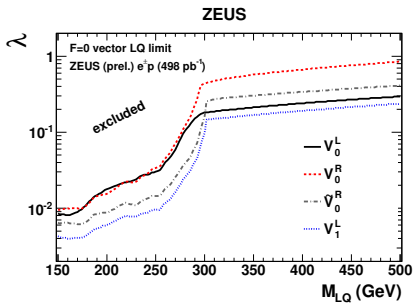

Figure 2: Preliminary exclusion curves for different first generation V-type LQs in the M_{LQ}-λ_{LQ}-plane from ZEUS. The areas above the lines are excluded at 95% C.L.

In the SM flavour changing neutral currents (*FCNC*) are strongly suppressed by the GIM mechanism. However there are extensions of the SM which predict FCNC contributions already at tree level. A possible signal for FCNC at HERA would be single top production $ep \to etX$. In the SM single top quarks are produced via the CC reaction $ep \to \nu tX$ with a cross section of less than 1 fb at HERA energies. A search for single top production is performed by ZEUS [15] with no signal above the CC background expectation being observed. In Fig. 3 the exclusion region in the plane of the top anomalous branching ratios $Br_{u\gamma}$ and Br_{uZ} from this analysis is shown together with results from other experiments. This analysis is able to extend the exclusion region at small $Br_{u\gamma}$ and Br_{uZ} values.

3 Diffraction

One of the big surprises observed at HERA at the beginning of the 90's was that about 10% of the events did not show any activity in the forward direction. These diffractive collisions, $ep \to eXp$, can be understood as resulting from processes in which the exchanged boson probes a colourless combination of partons from the proton.

To investigate the mechanism of diffraction two different methods are employed at HERA. Either the outgoing proton is directly detected in dedicated proton spectrometers, *FPS* or *LPS*, at very small angles in the direction of the proton beam and at large distance from the interaction region or a large gap in rapidity [3] (*LRG*) in the proton direction is required. The first method unambiguously identifies this process and enables the complete measurement of its kinematics but

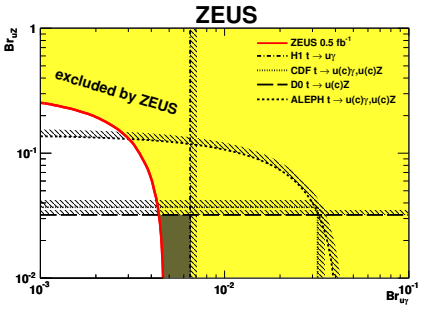

Figure 3: Exclusion boundary in the $Br_{u\gamma}$-Br_{uZ}-plane from ZEUS. The shaded region is excluded at 95% C.L.

[3] The rapidity is defined as $\eta = -\ln\tan\Theta/2$. The polar angle Θ is defined with respect to the proton direction.

suffers from small acceptance. The second method has large acceptance but also selects events with low mass excitations of the proton (proton dissociation).

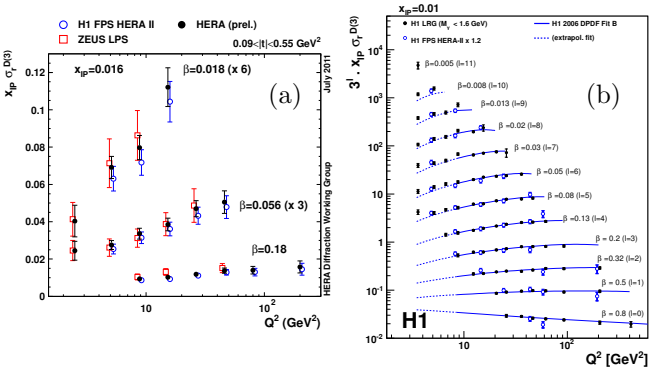

Figure 4: $x_{IP} \cdot \sigma_r^{D(3)}$ from (a) the preliminary HERA combined FPS/LPS data (black points) for $x_{IP} = 0.016$ compared to the uncombined data (open symbols) and (b) the H1 LRG data (black points) for $x_{IP} = 0.01$ in comparison to the H1 FPS data (open circles) corrected for contribution from proton dissociation.

For diffractive DIS (*DDIS*) in NC the QCD factorisation theorem holds [16], which allows DDIS to be described by diffractive PDFs (*DPDF*s) convoluted with hard scattering matrix elements. These DPDFs depend on four kinematic variables, namely the photon virtuality Q^2, the momentum transfer t at the proton vertex, the momentum fraction of the proton x_{IP} carried by the colourless exchange (*IP*) and the momentum fraction β of *IP* carried by the quark interacting with the photon. The latter two variables are related to Bjoken x via $x = x_{IP} \cdot \beta$.

The FPS and LPS DIS data measured by H1 and ZEUS have been combined using the same χ^2 minimisation procedure [17] as used previously for combining data at HERA [18]. In Fig. 4a the diffractive reduced cross section

$$\sigma_r^{D(3)}(x_{IP}, \beta, Q^2) = \frac{\beta Q^4}{2\pi\alpha_{em}^2} \frac{1}{1 - y + y^2/2} \frac{\mathrm{d}^3\sigma^{ep\to epX}}{\mathrm{d}x_{IP}\mathrm{d}\beta\mathrm{d}Q^2} = F_2^{D(3)} - \frac{y^2}{1 + (1-y)^2} F_L^{D(3)}, \quad (1)$$

with $y = Q^2/(sx)$, is shown for the preliminary HERA combined FPS/LPS data [19] for $x_{IP} = 0.016$ as a function of Q^2 and different values of β. In Eqn. 1 $F_2^{D(3)}$ and $F_L^{D(3)}$ denote the diffractive structure function and the diffractive longitudinal structure function, respectively. Also shown are the uncombined data. Due to cross calibration of the correlated systematic uncertainties of both experiments the combined data are more precise than expected from simple averaging. Scaling violations are evident from the change of the slope in Q^2 a function of β.

In Fig. 4b the diffractive reduced cross section $\sigma_r^{D(3)}$ from H1 [20] as measured by the LRG method based on the full HERA statistics is compared with pQCD predictions using the H1DPDF Fit B set [21]. The data are well described for $Q^2 > 10$ GeV^2. Also shown are the FPS measurements from H1 [22] scaled be a factor 1.20 to account for the proton dissociation contribution to the LRG data. The cross section measurements agree well with each other.

Using the LRG method H1 performed a direct measurement of the diffractive longitudinal structure function $F_L^{D(3)}$ [23]. This is the first measurement of F_L^D which became possible because of HERA running at reduced proton beam energies at the end of the HERA operation. In Fig. 5 the diffractive longitudinal structure function F_L^D divided by a parameterisation of the x_{IP} dependence of the reduced cross section $f_{IP/p}$ [21] is presented as a function of β for different Q^2. The pQCD predictions based on H1DPDF fit B included in the figure agree with data within uncertainties.

The NLO QCD analysis of inclusive DDIS cross section provides different solutions for the diffractive gluon density [21, 24]. This ambiguity can be resolved by studying diffractive di-jet production, which is directly sensitive to the diffractive gluon density [24, 25]. The H1 collaboration has performed the first measurement of the DDIS process $ep \to ejjX'p$ whit two jets and a leading proton in the final state. The differential cross section as a function of $\log_{10} x_{IP}$ is presented in Fig. 6 together with NLO QCD predictions based on the H1 DPDF fit B [21] and on the H1 2007 Jets [25] sets. Good agreement is observed between theory and data. In general the data are more precise than the predictions which have large scale uncertainties, as a measure for the importance of missing higher order contributions to the cross section.

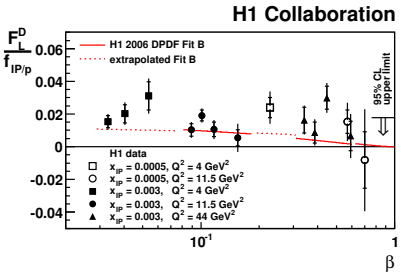

Figure 5: Diffractive longitudinal structure function F_L^D divided by a parameterisation of the x_{IP} dependence of the reduced cross section $f_{IP/p}$.

4 Jet Production

The study of jet production at HERA is very well suited for high precision measurements of the strong coupling constant α_S and to demonstrate its running over a large range in energy scale within a single experiment. Furthermore jet cross sections are valuable input for QCD analyses extracting proton PDFs because these data put significant constraints on the gluon density especially at medium x [26].

Inclusive jet production, $ep \to ejX$, is measured by ZEUS in the photoproduction regime (γp) where $Q^2 \approx 0$ for jet energies $E_T^{jet} > 17$ GeV [27]. The inclusive jet production cross section is shown in Fig. 7a as a function of η^{jet} in comparison to the NLO QCD expectation using the k_t jet algorithm [28]. In the lower part of the figure the ratio of the measured cross section to the NLO QCD calculation is shown. It is obvious that the theory does not describe the data well especially for forward η^{jet} where the prediction lies significantly below the data. This discrepancy may be resolved by either adding soft multiple interactions [29] to the theory or by using a different photon PDF set. In comparison to the data precision the theory uncertainties (hashed area) are very large mainly due to the scale variations used to estimate terms beyond NLO and due to the not well known photon PDFs. From these data the strong coupling constant is determined to be $\alpha_s(M_Z) = 0.120^{+0.0023}_{-0.0022}(exp.)^{+0.0042}_{0.0035}(th.)$. The analysis is also performed using the anti-k_t [30] and SIScone [31] jet algorithms. All results are found to be insensitive to the choice of the jet algorithm.

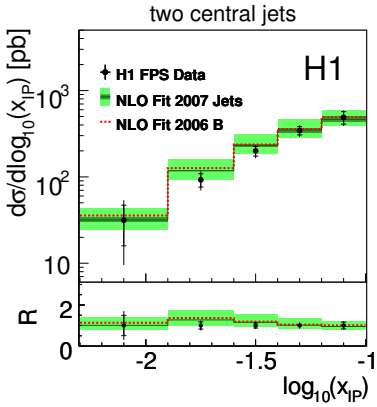

Figure 6: Diffractive dijet cross section as a function of $\log_{10} x_{IP}$ compared to NLO QCD predictions for two different DPDF sets. The theory uncertainties are indicated by the shaded band.

Normalised inclusive jet, dijet and trijet DIS cross sections for $Q^2 > 150$ GeV^2 from H1 [32] are presented in Fig 7b as a function of jet P_T for different values of Q^2. By the normalisation

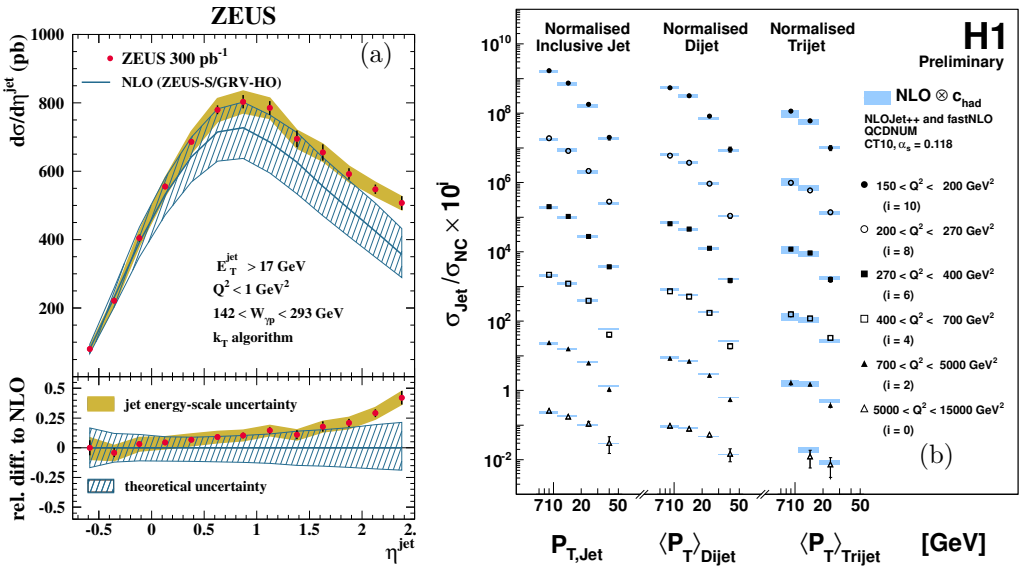

Figure 7: Jet production cross sections for (a) inclusive jet production in γp for $E_T^{jet} > 17$ GeV as a function of η^{jet} and (b) inclusive, dijet and trijet production in DIS normalised to the DIS cross section for $Q^2 > 150$ GeV^2 and $P_T^{jet} > 7$ GeV as a function of P_T for different Q^2.

to the inclusive DIS cross section the experimental systematic uncertainties are reduced. An unfolding technique is applied to properly account for correlations among the analysis bins and between the inclusive DIS, the inclusive jet, the dijet and the trijet sapmles.

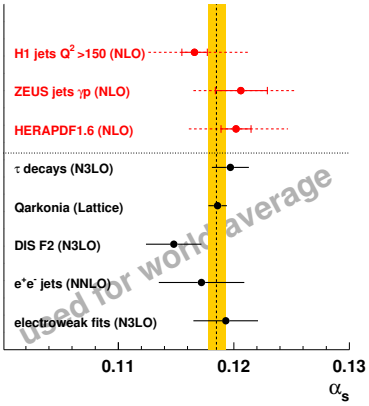

Figure 8: Compilation of α_S from different processes.

The data are also compared to NLO QCD prediction. The theory describes the data well over the full kinematic range. From these data the strong coupling constant α_S can be extracted. There is some tension observed when using the individual jet samples to determine α_S: the value obtained from the dijet sample is lower than that obtained from the other samples. This results in a poor χ^2 when fitting all samples together. The χ^2 improves significantly by restricting the phase space to the region where beyond NLO contributions are expected to be small. Using all three jet samples a value of $\alpha_S(M_Z) = 0.116 \pm 0.0011(exp.) \pm 0.0014(PDF) \pm 0.0008(had.) \pm 0.0039(theo)$ is obtained. As for jet production in γp the uncertainty on α_S is dominated by the uncertainty on the missing higher contributions.

In Fig. 8 these two α_S measurements and the preliminary result from the combined NLO QCD PDF+α_S fit to the inclusive and jet DIS data from HERA (*HERAPDF1.6*) are compared to the measurements used for the world average on α_S [7]. The HERA results are very consistent with the other measurements. The experimental uncertainties of the HERA results are comparable or superior to those from the other data apart from the error given for the lattice calculation. The precision

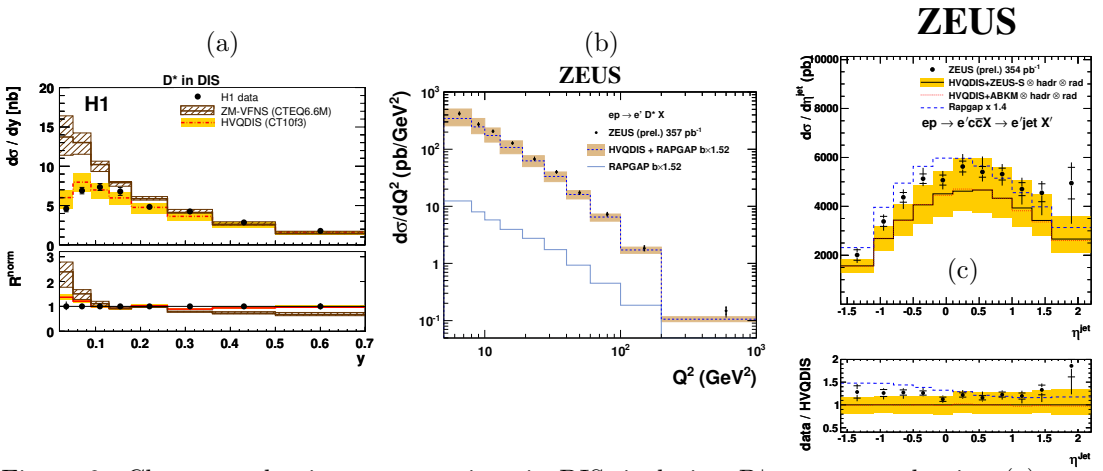

Figure 9: Charm production cross sections in DIS: inclusive D^* meson production (a) as a function of y (b) as a function of Q^2 and (c) charm jet production as a function of η^{jet}.

of the HERA data is spoiled by the theory uncertainties from missing higher orders.

5 Charm Production

The dominant process for charm production at HERA is photon-gluon-fusion, $\gamma g \to c\bar{c}$, which is sensitive to the gluon density in the proton. The charm contribution to the proton structure function F_2 rises up to 30% at larger Q^2. Therefore a good understanding of this process is vital for precision PDF determinations. Due to the relative large mass m_c of the charm quark pQCD is applicable without any phase space restrictions. However the presence of several hard scales (m_c, P_T^c and Q^2) makes this process to a multiple-scale problem. Depending on the relative magnitude of m_c, P_T^c and Q^2 different approaches on pQCD have been elaborated. Precision measurements of charm production allow for the validity of these approaches to be tested.

Different experimental methods are developed for tagging charm production. Results are presented based on $D^{*\pm}$ and D meson reconstruction and on charm tagging via secondary vertices which makes use of the longevity of charmed hadrons.

The D^* meson production cross sections in DIS are presented in Fig. 9a as a function of y as measured by H1 [33] and in Fig. 9b as a function of Q^2 as measured by ZEUS [34]. In Fig. 9c the charm jet cross section as a function of η^{jet} from ZEUS [35] is shown. Charm jets are identified by requiring the presence of a secondary vertex in the events well separated from the primary vertex with a reconstructed mass consistent with the expectation for charm jets.

The measurements are compared with NLO QCD calculations in the fixed-flavour-number-scheme (*FFNS*) [36] as implemented in the HVQDIS program [37]. The predictions for the different measurements agree well with the data. Also for charm production in DIS the experimental precision of the data is significantly superior to the precision of the theory which has large uncertainties dominated by the uncertainties attributed to the missing higher order contributions. The data in Fig. 9a are also compared to calculations in the zero-mass variable-flavour-number-scheme (*ZM-VFNS*) [38] which fails to describe the data. A similar observation

has been made in a previous publication on D^* meson production at high Q^2 [39]. Therefore this calculation is not appropriate for describing the charm contribution to the proton structure function.

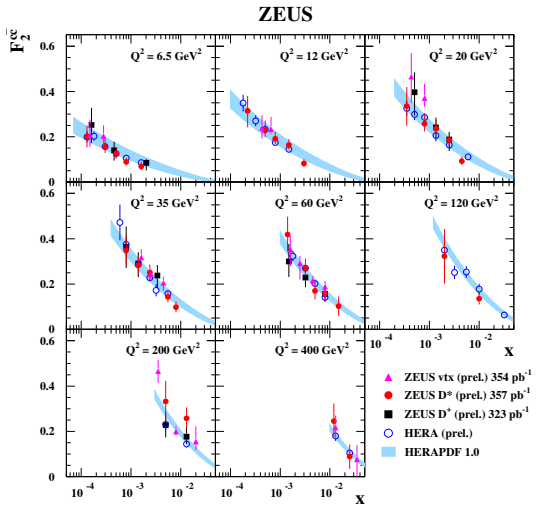

Figure 10: $F_2^{c\bar{c}}$ as a function of x for different values of Q^2 for the preliminary ZEUS measurements [34, 35] compared with the predictions based on HERAPDF1.0 (shaded band).

The measurements of charm production in DIS are used to determine the charm contribution $F_2^{c\bar{c}}$ to the proton structure function F_2. In Fig. 10 $F_2^{c\bar{c}}$ is shown as a function of x in bins of Q^2 extracted from the two preliminary ZEUS analyses discussed before. These data agree well with the preliminary HERA combined $F_2^{c\bar{c}}$ data [40]. Fig. 10 also includes the FFNS NLO QCD expectation based on HERAPDF1.0 [3] which is using only the inclusive HERA data as input. The uncertainty on the prediction is dominated by the uncertainty on m_c. The good description of the data by the calculation indicates that the gluon PDF in the proton tested by HERA processes is universal.

6 Particle Production

The study of particle production provides insight into both perturbative and non-perturbative aspects of QCD in parton fragmentation and hadronisation. The analyses of the fragmentation function into hadrons in different processes, i.e. in e^+e^-, pp or ep allows the universality of the fragmentation process to be tested.

At HERA only fragmentation into charged hadrons has been investigated so far [41, 42]. Here results from ZEUS on neutral strange particles are presented [43]. In Fig. 11a the K_s^0 scaled momentum spectrum observed in DIS is shown as a function of Q^2 in bins of x_p, with $x_p = 2P_{Breit}/Q$ and P_{Breit} being the momentum of the K_s^0 in the Breit frame[4]. Clear evidence for scaling violations is observed by the change of the Q^2 dependence from rising at small x_p to falling at large x_p. The data is compared with Monte Carlo (*MC*, lines) and with two NLO QCD calculations labeled AKK [44] and DSS [45] (shaded bands). While the MC expectations yield a fair description of the data AKK is significantly above the data except for $x_p > 0.6$ and DSS fails to describe the data for $x_p < 0.3$ at low Q^2. The better agreement of DSS may be related to the fact that this calculation is based on a global analysis of e^+e^-, pp and ep data while AKK uses e^+e^- data only. Similar deficits of the NLO QCD calculations have been observed for the charged particle production [41, 42].

In Fig. 11 new results on the production of very forward photons with $\eta_\gamma > 7.9$ in DIS from H1 [46] are also presented. These photons originate mainly from π^0 decays and therefore trace π^0 production at large η. In Fig. 11b the cross section for γ production normalised to the DIS cross section as a function of the transverse momentum p_T^{lead} of the leading photon is

[4]The Breit frame is defined as the frame in which the exchanged photon's 4-vector is (0,0,0,Q).

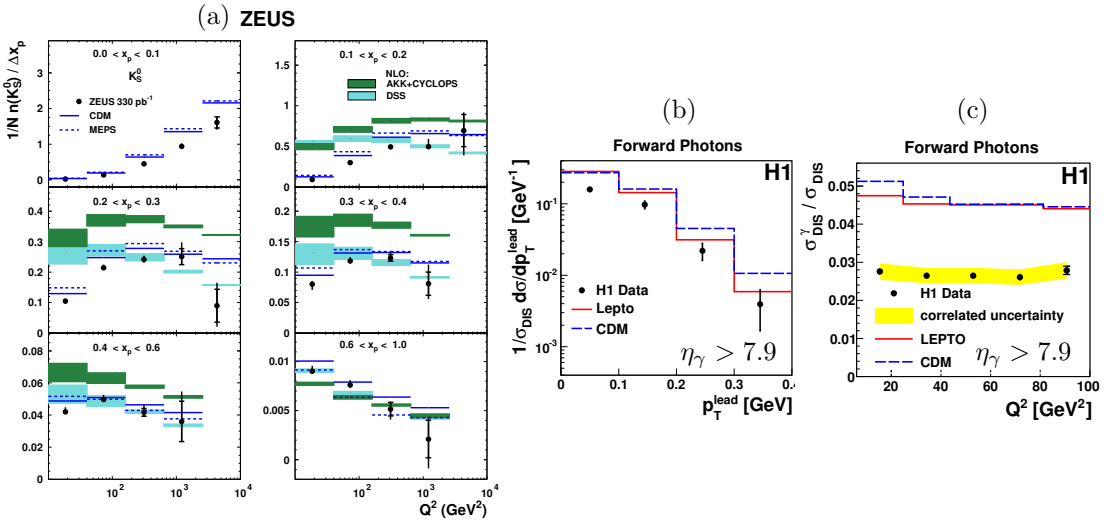

Figure 11: Particle production: (a) scaled momentum distribution for K_s^0 as a function of Q^2 in bins of x compared to MC and NLO QCD predictions, (b) normalised cross section for forward photon production as a function of p_T^{lead} and (c) forward photon yield as a function of Q^2.

compared to two MC calculations. Both MCs predict higher cross sections than observed in data suggesting that the fragmentation of spectator quarks (proton remnant) to π^0s is not well modelled. The yield $\sigma^{\gamma}_{DIS}/\sigma_{DIS}$ shown in FIg. 11c as a function of Q^2 is found to be consistent with being independent of Q^2 similar to what is observed in MC apart from normalisation. This observation is consistent with the expectation from the limiting fragmentation hypothesis which assumes the fragmentation of the spectator quarks to be independent of the kinematics of the hard interaction.

7 Conclusion

The QCD analyses at HERA have reached very high precision and may serve as acid test for theory. In general NLO QCD gives a fair to good description of the data with the exception of fragmentations where present NLO QCD calculations have difficulties in describing the data. Unfortunately the uncertainties of the theory attributed to the missing higher orders are almost everywhere much larger than the experimental errors. Not only the interpretation of the HERA data would profit from having next-to-next-to-leading order calculations for HERA processes but also the understanding of the data from hadron colliders would be facilitated since HERA is the backbone of any modern PDF.

References

[1] H.-L. Lai *et al.*, Phys. Rev. **D82** (2010) 074024 [arXiv:1007.2241].

[2] R. S. Thorne and R. G. Roberts ; Phys. Rev **D57** (1998) 6871; R. S. Thorne, Phys. Rev **D73** (2006) 054019 [hep-ph/0601245]; A. D. Martin *et al.* Eur. Phys. J. **C70** (2010) 51[arXiv:1007.2624].

[3] H1 and ZEUS Collab., F. D. Aaron *et al.* JHEP **1**(2010) 109 [arXiv:0911.0884].

[4] NNPDF Collab. R. D. Ball *et al.* [arXiv:1107.2652].
[5] S. Alekhin, J. Blümlein and S. Moch, S. Alekhin Phys. Rev **D81** (2010) 014032 [arXiv:0908.2766]; S. Alekhin, J. Blümlein and S. Moch [arXiv:12002.2281].
[6] I. Abt, this proceedings.
[7] A. Hoang, this proceedings.
[8] G. Altarelli, Phys. Rep. **81** (1982) 1.
[9] H1 and ZEUS Collab., H1prelim-11-042, ZEUS-prel-11-002.
[10] H1 Collab., F. D. Aaron *et al.*, Phys. Lett **B705** (2011) 52, [arXiv:1107.2478].
[11] H1 Collab., F. D. Aaron *et al.*, Phys. Lett **B704** (2011) 388, [arXiv:1107.3716].
[12] H1 Collab., F. D. Aaron *et al.*, Phys. Lett **B701** (2011) 20, [arXiv:1103.4938].
[13] ZEUS collab., ZEUS-prel-11-008; S. Antonelli, this proceedings.
[14] W. Buchmüller, R. Rückl and D. Wyler, Phys. Lett **B191** (1987) 442 [Erratum ibid. **B448** (1999) 320].
[15] ZEUS Collab., H. Abramowicz *et al.*, Phys. Lett **B708** (2011) 27 [arXiv:1111.3901].
[16] J. Collins, Phys. Rev. **D57** (1998) 3051 [Erratum ibid. **D61** (2000) 019902].
[17] A. Glazov, AIP Conf. Proc. **792** (2005) 237.
[18] H1 Collab. F. D. Aaron *et al.*, Eur. Phys. J. **C63**(2009) 625 [arXiv:0904.0929].
[19] H1 and ZEUS Collab., H1prelim-11-111, ZEUS-prel-11-011; V. Sola, this proceedings.
[20] H1 Collab., F. D. Aaron *et al.*, Eur. Phys. J. **C72** (2012) 1970 [arXiv:1203.4495].
[21] H1 Collab., A. Atkas *et al.*, Eur. Phys. J. **48** (2006) 715 [hep-ex/0606004].
[22] H1 Collab., F. D. Aaron *et al.*, Eur. Phys. J. **71** (2011) 1578 [arXiv:1010.1476].
[23] H1 Collab., F. D. Aaron *et al.*, Eur. Phys. J. **72** (2012) 1838 [arXiv:1107.3420].
[24] ZEUS Collab., S. Chekanov *et al.*, Nucl. Phys. **B831** (2010) 1 [arXiv:0911.4119].
[25] H1 Collab., A. Atkas *et al.*, JHEP 0710:42 [arXiv:0708.3217].
[26] H1 and ZEUS Collab., H1prelim-11-034, ZEUS-prel-11-001; K. Nowak this proceedings.
[27] ZEUS Collab., H. Abramowicz *et al.*, to be published in Nucl. Phys. **B** , arXiv:1205.6153.
[28] S. Catani *et al.*, Nucl. Phys. **B406** (1993) 187, S. D. Ellis and D. E. Soper, Phys. Rev. **D48** (1993) 3160.
[29] T. Sjöstrand and M. van Zijl, Phys. Rev. **D36** (1987) 2019.
[30] M. Cacciari, G. P. Salam and G. Soyez, JHEP **0804** (2008) 063 [arXiv:0802.1189].
[31] G. P. Salam and G. Soyez, JHEP **0705** (2008) 086 [arXiv:0704.0292].
[32] H1 Collab., H1prelim-12-031; D. Britzger this proceedings.
[33] H1 Collab., F. D. Aaron *et al.*, Eur. Phys. J. **71** (2011) 1769,[arXiv:1106.1028].
[34] ZEUS Collab., ZEUS-prel-11-012, A. Gizhko this proceedings.
[35] ZEUS Collab., ZEUS-prel-12-002, V. Libov this proceedings.
[36] E. Laenen *et al.*, Phys. Lett. **B291** (1992) 325; Nucl. Phys. **B392** (1993) 162; Nucl. Phys. **B392** (1993) 229; S. Riemersma *et al.*, Phys. Lett. **B347** (1995) 143 [hep-ph/0611029].
[37] B. Harris and J. Smith, Nucl. Phys. **B452** (1995) 109 [hep-ph/0611029]; Phys. Rev. **D57** (1998) 2806 [hep-ph/0611029].
[38] G. Heinrich and B. A. Kniehl, Phys. Rev. **D70** (2004) 094035,[hep-ph/0611029]; C. Sandoval, Proc. of XVII International workshop on Deep-Inelastic Scattering, Madrid, 2009 [arXiv:0908.0824];
[39] H1 Collab., F. D. Aaron *et al.*, Phys. Lett. **B686** (2010)91 [arXiv:0911.3989].
[40] H1 and ZEUS Collab., H1prelim-09-171, ZEUS-prelim-09-015.
[41] H1 Collab., F. D. Aaron *et al.*, Phys. Lett. **B654** (2007)148 [arXiv:0706.2456].
[42] ZEUS Collab., H. Abramowicz *et al.*, JHEP **6** (2010) 1 [arXiv:1001.4026].
[43] ZEUS Collab., H. Abramowicz *et al.*, JHEP **03** (2012) 020 [arXiv:1111.3526].
[44] S. Albino *et al.*, Phys. Rev. **D75** (2007) 034018 [hep-ph/0611029]; S. Albino, B. A. Kniehl and G. Kramer, Nucl. Phys. **B803** (2008) 42 [arXiv:0803.2768].
[45] D. de Florian, R. Sassot and M. Stratmann, Phys. Rev. **D75** (2007) 114010 [hep-ph/0703242].
[46] H1 Collab., F. D. Aaron *et al.*, Eur. Phys. J. **C71** (2011) 1771 [arXiv:1106.5944].